

Level density and γ -ray strength in $^{27,28}\text{Si}$

M. Guttormsen*, E. Melby, J. Rekstad, A. Schiller†, and S. Siem
Department of Physics, University of Oslo, N-0316 Oslo, Norway

T. Lönnroth
Department of Physics, Åbo Akademi, FIN-20500 Turku, Finland

A. Voinov

Frank Laboratory of Neutron Physics, Joint Institute of Nuclear Research, 141980 Dubna, Moscow reg., Russia

Primary γ -ray spectra are extracted by utilizing the $^{28}\text{Si}({}^3\text{He},\alpha\gamma)^{27}\text{Si}$ and $^{28}\text{Si}({}^3\text{He},{}^3\text{He}'\gamma)^{28}\text{Si}$ reactions. From a set of primary γ -spectra taken at excitation energies below the proton binding energy, a simultaneous extraction of the level density and the γ -ray transmission coefficient has been performed for the first time in this mass region. Typical nuclear temperatures are found to be $T \sim 2.4$ MeV at around 7 MeV of excitation energies. The entropy gap between nuclei with mass number A and $A \pm 1$ is measured to be $\delta S \sim 1.0k_B$, which indicates an energy spacing between single particle orbitals comparable with typical nuclear temperatures. The extracted γ -ray strength is also discussed.

PACS number(s): 21.10.Ma, 21.10.Pc, 24.10.Pa, 27.30.+t

I. INTRODUCTION

The Oslo Cyclotron group has developed a method to extract first-generation (primary) γ -ray spectra at various initial excitation energies [1]. From the set of primary spectra, nuclear level density and γ -ray strength function can be extracted [2,3]. These two functions reveal essential nuclear structure information such as shell-gaps, pair correlations and thermal and electromagnetic properties. In the last couple of years, the Oslo group has demonstrated several fruitful applications of the method [4–12].

So far the method has been tested on rare earth nuclei, having a rather uniform and high single particle level density. These properties are expected to be important for the foundation of the method. The two crucial steps in the extraction procedure are: (i) the subtraction technique for the primary γ -ray spectra, and (ii) the Brink-Axel hypothesis telling that nuclear resonances with approximately equal properties can be built on all states. Thus, the most important requirements are that the spin and parity distribution should be similar for all excitation bins, and that the nucleus should thermalize at each step within a given γ -cascade.

Although not finally validated, the method has been tested and found successful for deformed rare earth nuclei [4–11] and even for the weakly deformed $^{148,149}\text{Sm}$ nuclei [12]. However, in cases where the statistical properties are less favorable, as for lighter nuclei and/or for nuclei in the vicinity of closed shell, the foundation of the method is more doubtful. Since both ^{27}Si and ^{28}Si of the present study are open-shell systems, in the middle

of the sd shell, only the statistical question remains here.

In this work we have tested the extraction procedure on the light ^{27}Si and ^{28}Si systems applying the $({}^3\text{He},\alpha)$ pick-up reaction and the $({}^3\text{He},{}^3\text{He}')$ inelastic scattering reaction, respectively. Since both the level density and the γ -decay rates are known in these nuclei, a quantitative judgment of the applicability of the procedure is feasible. Section II describes the experimental methods and techniques, and in Sects. III and IV the level density and γ -ray strength are discussed. Finally, concluding remarks are given in Sect. V.

II. EXPERIMENTAL METHOD AND TECHNIQUES

The experiment was carried out at the Oslo Cyclotron Laboratory with a 45 MeV ${}^3\text{He}$ beam. The self-supporting ^{28}Si target was isotopically enriched to 100% and had a thickness of 3 mg/cm². The reactions employed in the extraction procedure were $^{28}\text{Si}({}^3\text{He},\alpha\gamma)^{27}\text{Si}$ and $^{28}\text{Si}({}^3\text{He},{}^3\text{He}'\gamma)^{28}\text{Si}$.

The charged particles and γ rays were recorded with the detector array CACTUS, which contains eight particle telescopes, 27 NaI γ -ray detectors and two additional Ge detectors monitoring the spin distribution and the selectivity of the reactions. Each telescope is placed at an angle of 45° relative to the beam axis, and comprises one Si front and one Si(Li) back detector with thickness 140 and 3000 μm , respectively. The NaI γ -detector array surrounding the target and particle detectors, has a

*Electronic address: magne.guttormsen@fys.uio.no

†Present address: Lawrence Livermore National Laboratory, L-414, 7000 East Avenue, Livermore CA-94551

resolution of $\sim 6\%$ at $E_\gamma = 1$ MeV and a total efficiency of $\sim 15\%$.

In Figs. 1 and 2 the single and coincidence ejectile spectra are shown for the reactions $^{28}\text{Si}({}^3\text{He},\alpha)^{27}\text{Si}$ and $^{28}\text{Si}({}^3\text{He},{}^3\text{He}')^{28}\text{Si}$, respectively. The ground state in ^{27}Si is located at higher ejectile energy due to a positive Q -value of 3.40 MeV in the $({}^3\text{He},\alpha)$ reaction. In ^{27}Si and ^{28}Si , pronounced peak-structures are seen up to 5 and 10 MeV of excitation energy, respectively. The coincident spectra show a drop in yield at the proton binding energies B_p , since the residual nucleus with one proton less (aluminum) is then populated at low excitation energy with a corresponding low γ -ray multiplicity. Our extraction method is therefore only applicable up to the excitation energy of $E \sim B_p$.

In order to determine the true γ -energy distribution, the γ spectra are corrected for the response of the NaI detectors with the unfolding procedure of Ref. [13]. In addition random coincidences are subtracted from the γ -spectra. The resulting unfolded NaI γ -spectra are shown in Fig. 3. The spectra reveal strong γ -lines, which are identified as transitions between low-lying states.

The set of unfolded γ -spectra are organized in a (E, E_γ) matrix, where the initial excitation energies E of ^{27}Si and ^{28}Si are determined by means of reaction kinematics utilizing the energy of the ejectile. This matrix comprises the γ -energy distribution of the total γ cascade. The primary γ matrix can now be found according to the subtraction technique of Ref. [1].

As indicated in the introduction, the primary γ -ray procedure is based on the assumption that the decay properties of the particular reaction-selected distribution of states within each energy bin are independent on whether the respective ensembles of states are directly populated through the nuclear reaction or by γ -decay from higher lying states. In the present case the γ -ray multiplicity is low and reaches $M_\gamma \sim 2$ around 10 MeV of excitation energy. Thus, generally less than half of the counts in the total γ spectra have to be subtracted in the procedure, giving quite reliable primary γ -ray spectra. This is demonstrated in Fig. 4 where we compare our results with known γ -decay branches from various excitation regions [14]. Taking into account that probably not all levels and branchings are known, the agreement is very satisfactory.

The idea is now to find two functions, the level density $\rho(E)$ and the γ -energy dependent function $F(E_\gamma)$, that multiplied with each other reproduce the set of primary γ -ray spectra. The $F(E_\gamma)$ function is identified as the so-called γ -ray transmission coefficient. According to the Brink-Axel hypothesis [15,16] the primary γ -ray spectra can be factorized by

$$P(E, E_\gamma) \propto \rho(E - E_\gamma) F(E_\gamma), \quad (1)$$

where $P(E, E_\gamma)$ is fitted to the primary γ -ray matrix by a least χ^2 fit [3]. In the factorization procedure we use primary spectra from the initial excitation regions of

$E = 3.6 - 7.6$ MeV and $E = 4.2 - 12.1$ MeV for ^{27}Si and ^{28}Si , respectively. The corresponding γ -regions were chosen to be $E_\gamma = 1.1 - 7.6$ MeV and $E_\gamma = 2.2 - 12.1$ MeV.

In Fig. 5 the best fits (solid lines) to the experimental P are shown for the ^{27}Si and ^{28}Si nuclei. The spectra exhibit strong peak structures that are seen to be fairly well described by the factorization in Eq. (1). From the multiplicative functions ρ and F , one can construct an infinite number of other functions [3] which give identical fits to the data of Fig. 5 by

$$\tilde{\rho}(E - E_\gamma) = A \exp[\alpha(E - E_\gamma)] \rho(E - E_\gamma), \quad (2)$$

$$\tilde{F}(E_\gamma) = B \exp(\alpha E_\gamma) F(E_\gamma). \quad (3)$$

Consequently, neither the slope nor the absolute value of the two functions can be obtained through the fitting procedure. The free parameters A , B and α have to be determined from other information to give the best physical solution.

III. LEVEL DENSITY

The ^{27}Si and ^{28}Si nuclei have been thoroughly studied during the last decades, and the level schemes are probably fairly complete up to several MeV of excitation energy. By smoothing the known level density taken from the database of Ref. [14] with the experimental energy resolution, we can adjust the parameters A and α of our experimental ρ to fit the density based on known levels. The adjustments were performed at $E = 0.9$ and 5.0 MeV in ^{27}Si and at $E = 1.7$ and 7.0 MeV in ^{28}Si . These anchor points are well determined and separated in excitation energy, however, also other data points could as well be used.

Figure 6 shows the comparison between our data (data points) and known levels [14]. Also the results of smoothing the known levels on excitation energy are shown (solid curve). The overall agreement is gratifying. Local differences can be caused by violation of the Axel-Brink hypotheses for light nuclei where low level density and large fluctuations of γ intensity is observed. For example, in ^{28}Si the density around the ground state is strongly underestimated in our experiment, because very few transitions decay directly to the $I^\pi = 0^+$ ground state. This property is less pronounced in ^{27}Si having a ground state assignment of $I^\pi = 5/2^+$. Since these nuclei have been well studied, we are not able to extract much more information on the level density than what is already known. However, our data give a small indication that not all levels in ^{28}Si have yet been observed above 9 MeV of excitation energy.

Very few explicit calculations of level densities exist. This would be needed since a simple Fermi-gas approximation based on the level density parameter a and the pairing gap parameter Δ neglects residual interactions.

In the calculations of Ormand *et al.* [17], the level densities of ^{24}Mg and ^{32}S were studied in a Monte Carlo Shell-Model approach within the sd shell. It is interesting that the level density in ^{24}Mg behaves very much like the nuclei studied here. The fact that there are only hundred levels per MeV at excitation energies of 8 – 12 MeV has implications. It indicates that if specific states are selected by some reaction, e.g. α -cluster states with large parentage of $\pi^2\nu^2$ configurations, the number of states of this kind necessarily must be significantly lower. However, at this stage it is not possible to give quantitative statements of the number of e.g. α -cluster states in this region.

In general, the most successful way to create additional states in atomic nuclei is to break up $J = 0$ nucleon Cooper pairs from the core. Each broken pair gives 10 – 20 times more states, which is much higher than obtained from other modes of excitation, as rotation or vibration. Recently [18,19], a thermodynamic model was developed which could describe level densities for mid-shell nuclei in the mass regions $A = 58, 106, 162$ and 234 . The model is based on the canonical ensemble theory where equilibrium is obtained at a certain given temperature T .

The basic idea of the model [18,19] is the assumption of a reservoir of proton and neutron pairs. The pairs may be broken so that unpaired nucleons are thermally scattered into an infinite, equidistant, doubly degenerated single-particle level scheme. In addition, rotational and vibrational modes may be thermally excited. The total partition function is written as a product of proton (Z_π), neutron (Z_ν), rotation (Z_{rot}) and vibration (Z_{vib}) partition functions. Then, from the Helmholtz free energy

$$F(T) = -T \ln (Z_\pi Z_\nu Z_{\text{rot}} Z_{\text{vib}}), \quad (4)$$

thermodynamical quantities as entropy, average excitation energy and heat capacity can be calculated as

$$S(T) = - \left(\frac{\partial F}{\partial T} \right)_V \quad (5)$$

$$\langle E(T) \rangle = F + ST \quad (6)$$

$$C_V(T) = \left(\frac{\partial \langle E \rangle}{\partial T} \right)_V, \quad (7)$$

where the Boltzmann constant is set to unity ($k_B = 1$) and the temperature T is measured in MeV. The level density is calculated applying the saddle-point approximation [20]

$$\rho(\langle E \rangle) = \frac{\exp(S)}{T \sqrt{2\pi C_V}}. \quad (8)$$

¹The proton and neutron parameters are identical and give no difference between odd-even and even-odd systems. We therefore denote either of these two systems as the odd- A system.

The energy spacing between the single particle orbitals ε is the most critical parameter of the model. In order to determine ε , we compare with the well studied ^{26}Al and ^{27}Al isotopes, where the level density is presumably known up to high excitation energy from the counting of experimentally observed levels [14]. Figure 7 shows these experimental data together with a level density point evaluated for ^{28}Al [9] from the average neutron resonance spacing [21] at the neutron binding energy B_n . The slopes of the level densities are well reproduced with $\varepsilon = 2.0$ MeV, which is consistent with the energy gaps in the Nilsson single particle level scheme. The difference in level density between ^{26}Al and ^{27}Al depends strongly on the pairing gap energy and is well described with a gap parameter of $\Delta = 12A^{-1/2}$ MeV = 2.3 MeV, using $A = 28$. The pairing attenuation factor, defined as the ratio between the amount of energy needed to break one nucleon pair compared to the previous broken pair, is set to $r = 0.56$ (for details see Ref. [19]). For simplicity, we have used the same values of ε , Δ and r for protons and neutrons. Furthermore, all calculations include a reservoir of seven proton and seven neutron pairs. The collective parameters are taken from experimental data on ^{28}Si . The rotational parameter $A_{\text{rot}} = E/2(2+1) = 0.3$ MeV is calculated from the first excited state ($I^\pi = 2^+$), and the vibrational energy $\hbar\omega_{\text{vib}} = 5.0$ MeV is set equal to the excitation energy of the first non-rotational state ($I^\pi = 0^+$).

The very same parameter set is used in the calculation for ^{27}Si and ^{28}Si in Fig. 8. The calculation fits well the experimental data of ^{27}Si for excitation energies above $E \sim 4$ MeV. For ^{28}Si , the more statistical and smooth part of the level density takes place first above $E \sim 9$ MeV, where the model describes the data fairly well.

By comparing the level densities between even-even (^{28}Si), odd- A (^{27}Al or ^{27}Si) and odd-odd (^{26}Al) systems¹, we may extract interesting information. In Fig. 9 the free energy F , entropy S , average excitation energy $\langle E \rangle$ and heat capacity C_V are shown as function of temperature for the three systems. A fruitful quantity is the entropy gap δS between systems with A and $A \pm 1$. At low temperatures this quantity is approximately extensive (additive) and represents the single particle entropy associated with the valence particle (or hole) [9]. In the upper right panel, we find that the nucleon carries a single particle entropy of $\delta S \sim 1.0$ at $T \sim 1.5$ MeV.

The single particle entropy can also be deduced from the experimental data of aluminum (and possibly also

from silicon). The high energy data points of Fig. 7 reveal that the level density for ^{26}Al is ~ 2.7 times higher than for ^{27}Al . Remembering that the level density and entropy is connected by

$$S = \ln \rho + \text{constant}, \quad (9)$$

we deduce also here $\delta S \sim 1.0$.

The statistical definition of temperature in the micro-canonical ensemble is given by

$$T = \left(\frac{\partial S}{\partial E} \right)_V^{-1}, \quad (10)$$

giving typically $T \sim 2.4$ MeV for the data points of ^{27}Al in the excitation region of $7 - 11$ MeV, see Fig. 7. Since the excitation energy shift between the level densities of Fig. 7 amounts approximately to the pairing gap parameter Δ , we may express the slope of $\ln(\rho)$ as $\delta S/\Delta$ or, according to Eqs. (9) and (10), as T^{-1} giving

$$\delta S = \Delta/T, \quad (11)$$

which again confirms $\delta S = 2.3/2.4 \sim 1.0$.

The extracted single particle entropy is lower than observed in heavier mid-shell nuclei where typically $\delta S \sim 1.7$ [9]. The recent findings are supported by the systematics of Fig. 10, where the experimentally deduced level densities at $E = 7$ MeV are displayed for various nuclear systems. For mass numbers below $A \sim 40$ the level densities drop one order of magnitude, and the density gaps between the various systems are severely reduced. From our model calculations, this change is due to a decrease in the ratio between the temperature T and the single particle level energy spacing ε . In the mass region studied here, the temperature and spacing is approximately equal, i.e. $T \sim \varepsilon$, and the valence nucleon is thermally smeared over the ground state and first excited single particle level, giving $\delta S = \ln 2 = 0.7$, only. In the rare earth region, we have typically $T \sim 3\varepsilon$ and the valence nucleon is thermally spread over several single particle levels, giving higher entropy.

The heat capacity curves of Fig. 9 show S-shaped forms, in particular for the even-even system. The local maximum of this shape appears at $T_m \sim 2.4$ MeV, corresponding to an excitation energy of $\langle E \rangle = 10$ MeV. At this point the excitation energy increases strongly with temperature signalizing a substantial depairing process. It is tempting to connect this overshoot in heat capacity with a pairing phase transition. In order to test this, we have studied the distribution of zeros of the partition function in the complex temperature plane, as prescribed in Refs. [19,22]. In our calculations we find that the zeros move away from the real inverse temperature axis with

increasing inverse temperature. This property is inconsistent with a pairing phase transition in the thermodynamical limit of $A \rightarrow \infty$, in accordance with the generalized Ehrenfest definition of a phase transition [23]. A similar conclusion has also been drawn in the Fe region [19].

IV. GAMMA-RAY STRENGTH

The γ -ray energy dependent function $F(E_\gamma)$ contains information on the average γ -decay probability. In Fig. 11 the non-normalized $F(E_\gamma)$ of Eq. (3) is shown with the α parameter determined in Sect. III. The two extreme data points at $E_\gamma = 3.2$ and 5.0 MeV for ^{27}Si and ^{28}Si , respectively, are probably due to a singularity in the extraction method giving too small error bars.

It has been shown [24,25] that the regularity of the γ -decay strength in continuum is determined by the γ -ray strength function²

$$f_{XL} = \Gamma_{XL}^i(E_\gamma)/(E_\gamma^{2L+1} D^i), \quad (12)$$

where E_γ is the transition energy, X is the electric or magnetic character, L is the multipolarity, $\Gamma_{XL}^i(E_\gamma)$ is the partial radiative width and D^i is the level spacing of the initial states i with equal spin and parity. The main part of high lying levels is known to decay by E1 and M1 γ transitions. Thus, one could in principle extract $f_{E1} + f_{M1}$ from the present experiment in the same way as has been done for several rare earth nuclei [10–12]. However, the concept of an average radiative width is difficult to adopt for these light nuclei since the average level spacing D^i is highly uncertain; there are less than one level per MeV with presumably the same spin and parity.

Even though the absolute strength of f is uncertain, its functional dependency on E_γ can be studied. The shape of the measured γ -ray transmission coefficient F is given by

$$F(E_\gamma) \propto [f_{E1}(E_\gamma) + f_{M1}(E_\gamma)] E_\gamma^3, \quad (13)$$

for dipole transitions. If the transitions are mainly governed by single particle transitions, an E_γ^3 shape would be expected according to the Weisskopf estimate. This functional form is displayed in Fig. 11. Both ^{27}Si and ^{28}Si show a rather flat F shape for $E_\gamma < 4 - 5$ MeV. However, for $E_\gamma > 4 - 5$ MeV ^{28}Si follows roughly the E_γ^3 dependency, indicating that the transitions are rather of single particle than collective origin as found for rare earth nuclei [10–12]. Also the large spread in lifetimes [14] of the high lying levels supports this interpretation.

²Also called the radiative strength function in literature.

V. CONCLUSIONS

A simultaneous extraction of level densities and γ -ray transmission coefficients in $^{27,28}\text{Si}$ has been performed. This study demonstrates that the extraction method also works for light nuclei, despite the fact that thermalization might seem questionable. The concept of a γ -ray strength function in this mass region is not very useful. The measured γ -energy dependence of approximately E_γ^3 indicates that the γ decay is governed by single particle dipole transitions.

A simple thermodynamical model reproduces the high excitation region of the experimental data. From the data on $^{27,28}\text{Si}$ and $^{26,27}\text{Al}$ we extract a common nuclear temperature of $T \sim 2.4$ MeV and pairing gap of $\Delta \sim 2.3$ MeV. Both experiment and model indicate that the valence nucleon in these systems carries an entropy of $\delta S \sim 1.0$. This is close to the expected value of 0.7 when the thermal nucleonic excitation is smeared over the ground state and only one excited single particle level. The pair breaking process is strongly smeared out in temperature (and excitation energy), and a phase transition in the sense of the Ehrenfest definition is doubtful.

The present work encourages also similar nuclear studies in the mass region $A = 30 - 100$ where level density and γ -strength function play an important role in the nucleosynthesis of stellar objects.

ACKNOWLEDGMENTS

Financial support from the Norwegian Research Council (NFR) is acknowledged. T. Lönnroth and A. Voinov warmly acknowledge the financial support from the Magnus Ehrnrooth Foundation in Helsinki and a NATO fellowship grant, respectively.

- [1] M. Guttormsen, T. Ramsøy, and J. Rekstad, Nucl. Instrum. Methods Phys. Res. A **255**, 518 (1987).
- [2] L. Henden, L. Bergholt, M. Guttormsen, J. Rekstad, and T.S. Tveter, Nucl. Phys. **A589**, 249 (1995).
- [3] A. Schiller, L. Bergholt, M. Guttormsen, E. Melby, J. Rekstad, and S. Siem, Nucl. Instrum. Methods Phys. Res. A **447** 498 (2000).

- [4] E. Melby, L. Bergholt, M. Guttormsen, M. Hjorth-Jensen, F. Ingebretsen, S. Messelt, J. Rekstad, A. Schiller, S. Siem, and S.W. Ødegård, Phys. Rev. Lett. **83**, 3150 (1999).
- [5] A. Schiller, M. Guttormsen, E. Melby, J. Rekstad, and S. Siem, Phys. Rev. C **61**, 044324 (2000).
- [6] M. Guttormsen, M. Hjorth-Jensen, E. Melby, J. Rekstad, A. Schiller, and S. Siem, Phys. Rev. C **61**, 067302 (2000).
- [7] M. Guttormsen, A. Bjerve, M. Hjorth-Jensen, E. Melby, J. Rekstad, A. Schiller, S. Siem, and A. Belić, Phys. Rev. C **62**, 024306 (2000).
- [8] A. Schiller, A. Bjerve, M. Guttormsen, M. Hjorth-Jensen, F. Ingebretsen, E. Melby, S. Messelt, J. Rekstad, S. Siem, and S.W. Ødegård, Phys. Rev. C **63**, 021306 (2001).
- [9] M. Guttormsen, M. Hjorth-Jensen, E. Melby, J. Rekstad, A. Schiller, and S. Siem, Phys. Rev. C **63**, 044301 (2001).
- [10] E. Melby, M. Guttormsen, J. Rekstad, A. Schiller, S. Siem, Phys. Rev. C **63**, 044309 (2001).
- [11] A. Voinov, M. Guttormsen, E. Melby, J. Rekstad, A. Schiller, and S. Siem, Phys. Rev. C **63**, 044313 (2001).
- [12] S. Siem, M. Guttormsen, E. Melby, J. Rekstad, A. Schiller, and A. Voinov, Phys. Rev. C, to be published and preprint nucl-ex/0111012.
- [13] M. Guttormsen, T.S. Tveter, L. Bergholt, F. Ingebretsen, and J. Rekstad, Nucl. Instrum. Methods Phys. Res. A **374**, 371 (1996).
- [14] Data extracted using the NNDC On-Line Data Service from the ENSDF database, file revised as of Jan. 21, 2000.
- [15] D.M. Brink, Ph.D. thesis, Oxford University (1955).
- [16] P. Axel, Phys. Rev. **126**, 671 (1962).
- [17] W.E. Ormand, Phys. Rev. C **56**, R1678 (1997).
- [18] M. Guttormsen, M. Hjorth-Jensen, E. Melby, J. Rekstad, A. Schiller, and S. Siem, Phys. Rev. C **64**, 034319 (2002).
- [19] A. Schiller, M. Guttormsen, M. Hjorth-Jensen, J. Rekstad, and S. Siem, preprint nucl-ex/02xxxyy.
- [20] H. Nakada and Y. Alhassid, Phys. Rev. Lett. **79**, 2939 (1997).
- [21] A.S. Iljinov, M.V. Mebel, N. Bianchi, E. De Sanctis, C. Guaraldo, V. Lucherini, V. Muccifora, E. Polli, A.R. Reolon, and P. Rossi, Nucl. Phys. **A543**, 517 (1992).
- [22] D. Chowdhury and D. Stauffer, *Principles of Equilibrium Statistical Mechanics* (Wiley-VCH, D-69469 Weinheim, 2000) p.285.
- [23] P. Ehrenfest, Leiden Commun. Suppl. **75b** (1933); Proc. Akad. Wet. **36**, 153 (1933).
- [24] J.M. Blatt and V.F. Weisskopf, *Theoretical Nuclear Physics* (John Wiley & Sons, New York, 1952).
- [25] G.A. Bartholomew, E.D. Earle, A.J. Ferguson, J.W. Knowles, and M.A. Lone, Adv. Nucl. Phys. **7**, 229 (1973).

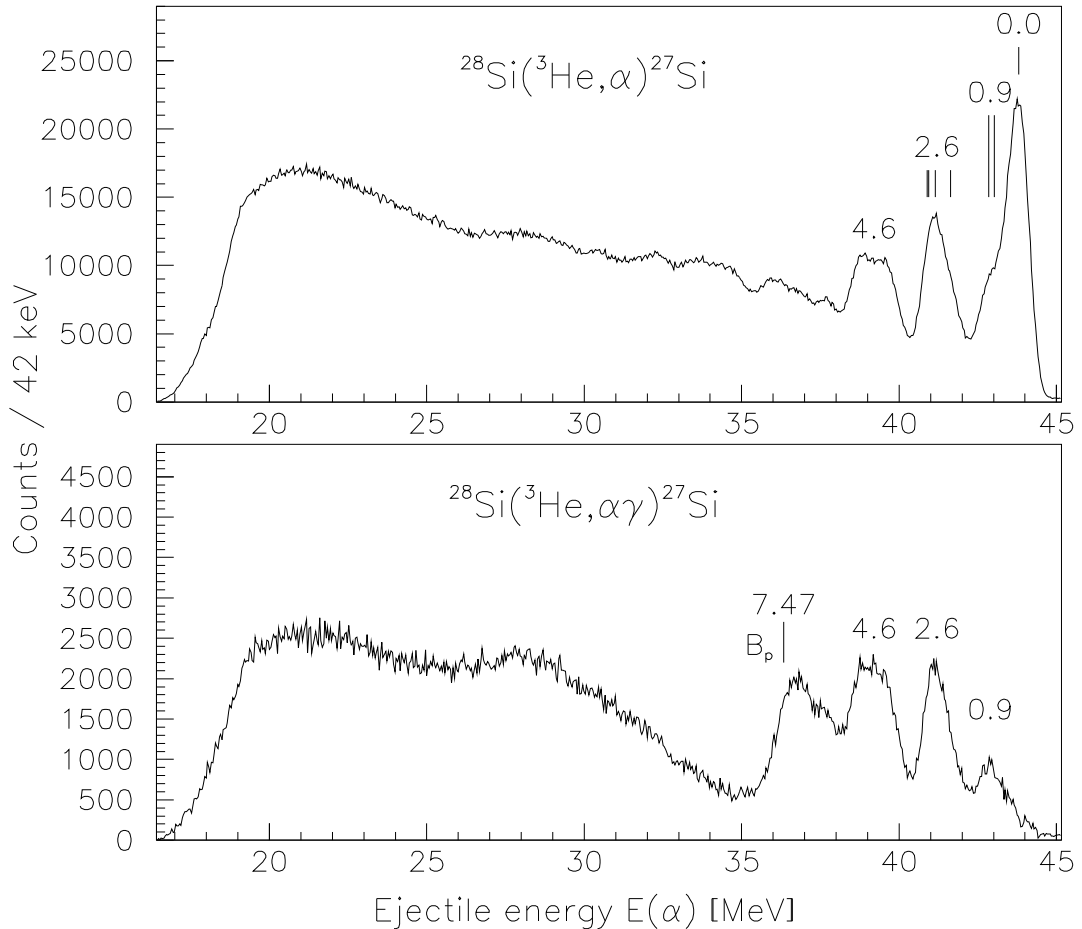


FIG. 1. α -particles from the $^{28}\text{Si}({}^3\text{He}, \alpha)$ reaction measured in 45° with respect to the beam axis and with a beam energy of 45 MeV. The lower panel shows the same spectrum, but in coincidence with one or more γ rays detected in the NaI detectors. Some known levels and the proton binding energy are indicated in MeV and by vertical lines.

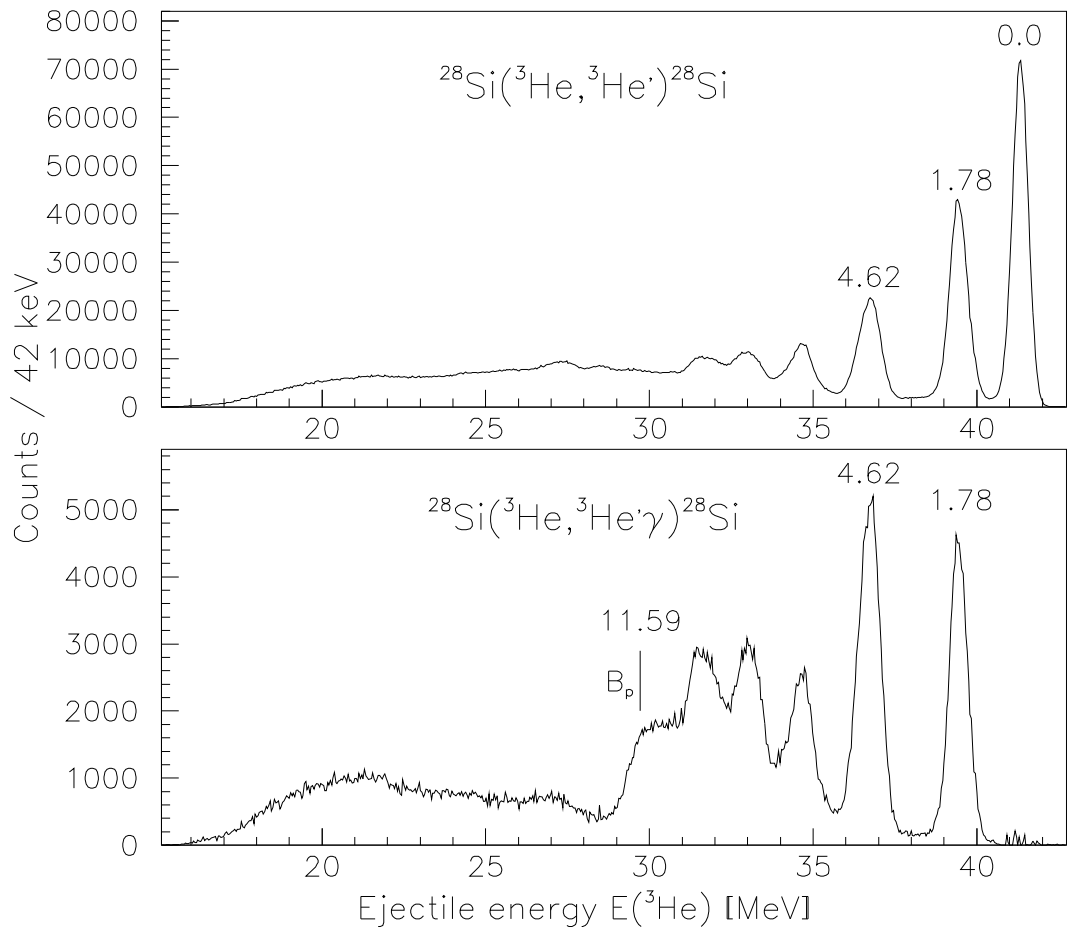


FIG. 2. Same as Fig. 1, but ${}^3\text{He}$ -particles from the ${}^{28}\text{Si}({}^3\text{He}, {}^3\text{He}')$ reaction.

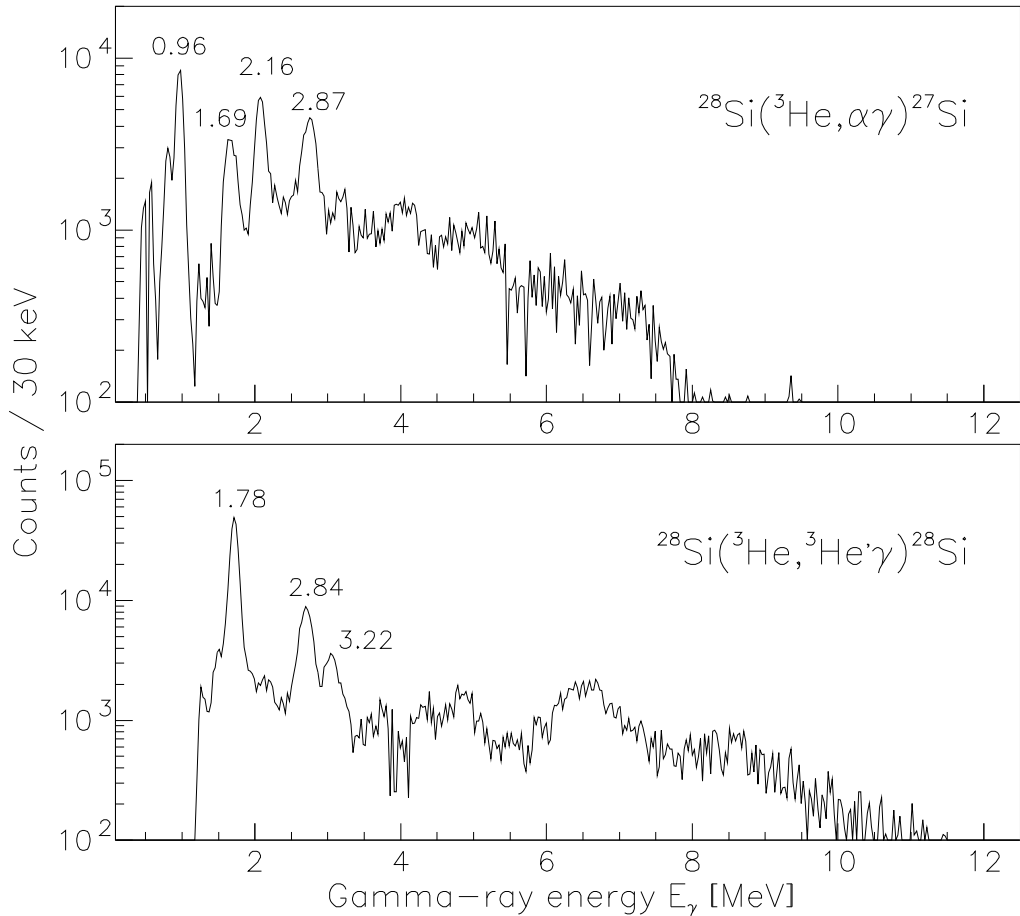


FIG. 3. Unfolded NaI γ -ray spectra from ^{27}Si and ^{28}Si . The strongest γ lines are indicated by energies in MeV.

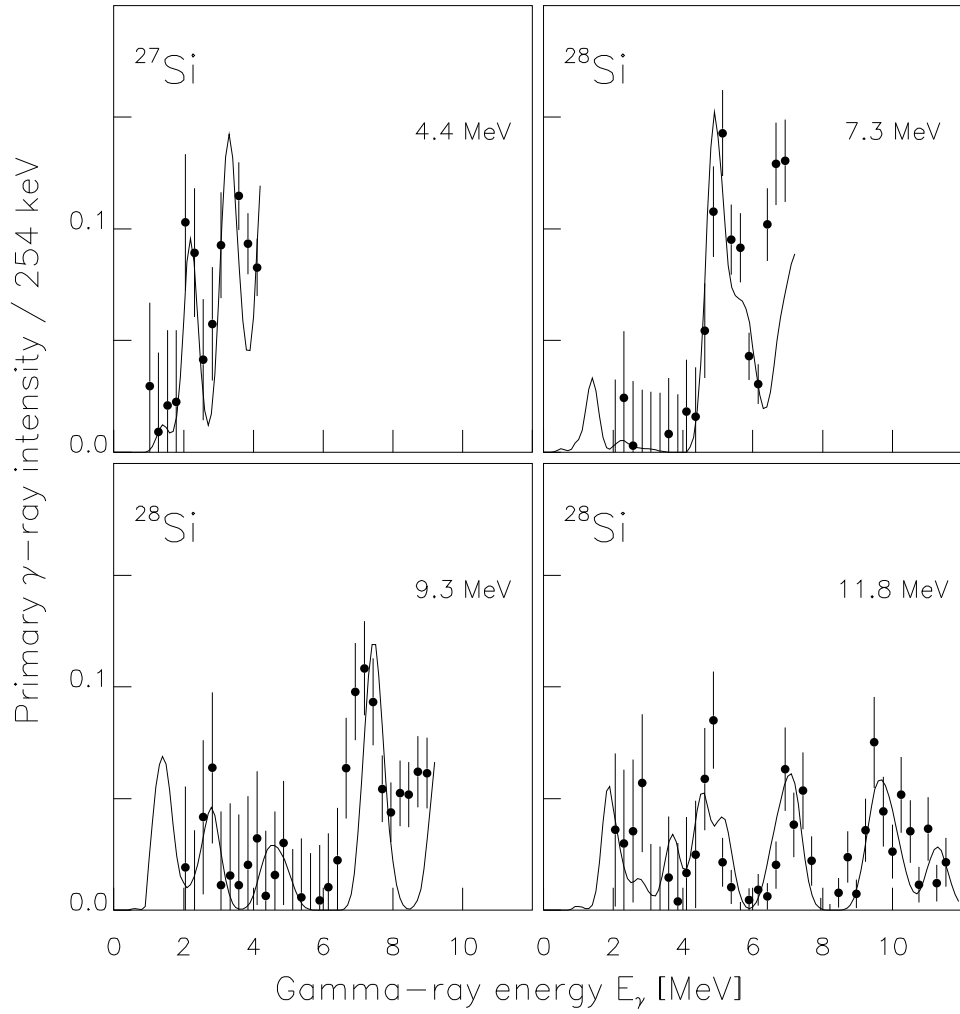


FIG. 4. Comparison between primary γ -ray spectra extracted with our method (data points with error bars) and the spectra (solid lines) constructed from the known [14] γ -decay branching of levels around excitation energies indicated for each panel. The spectra are normalized to unity.

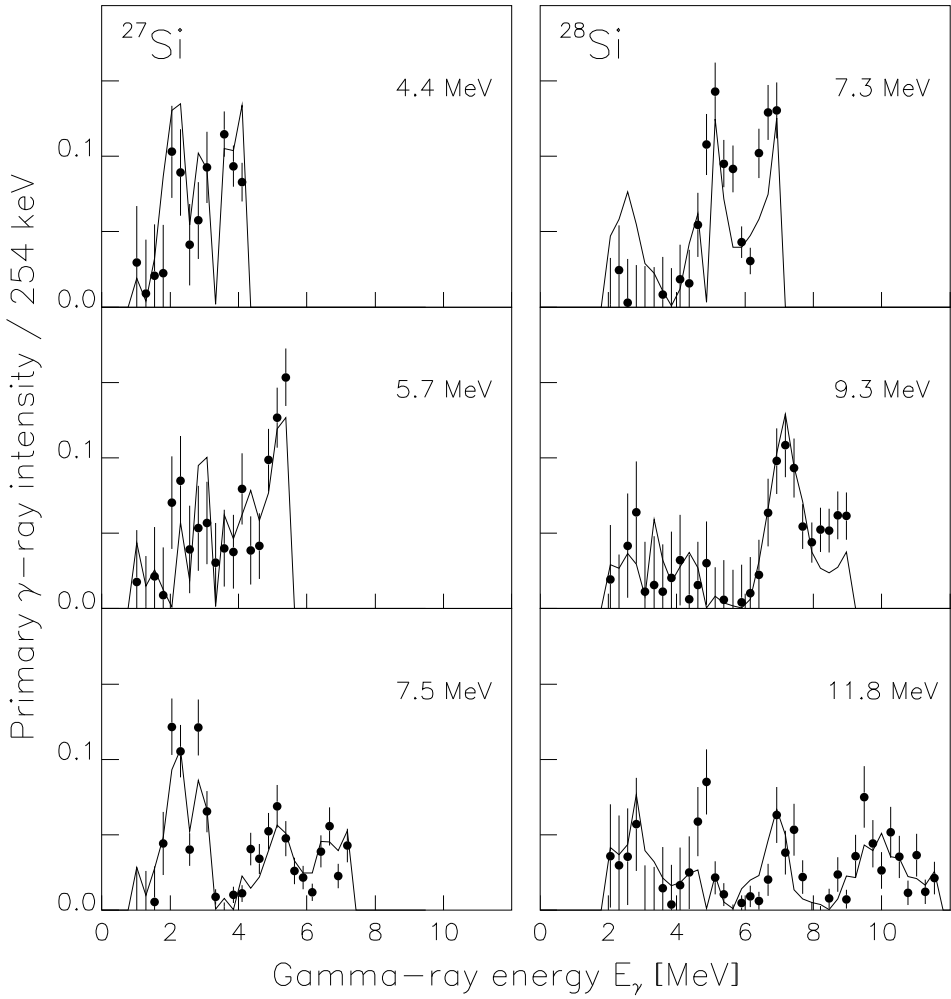


FIG. 5. Comparison between experimental primary γ -ray spectra (data points with error bars) and the distribution (solid lines) calculated from the extracted level density $\rho(E)$ and the γ -ray transmission coefficient $F(E_\gamma)$. The initial excitation energy bins are indicated in each panel. The spectra are normalized to unity.

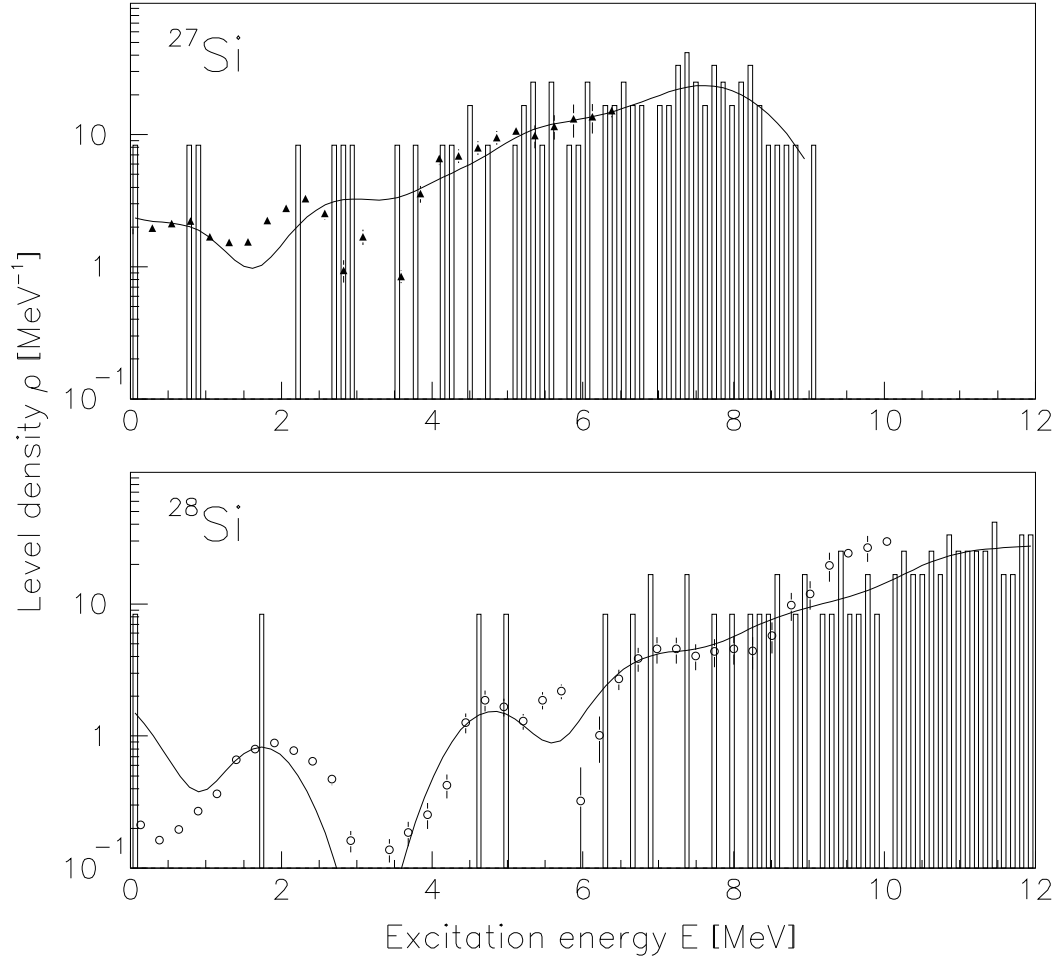


FIG. 6. Extracted level densities (data points with error bars) in ^{27}Si and ^{28}Si compared with the density of known levels (histogram). The solid curve is obtained by smoothing the known level density by a Gaussian with FWHM = 1.1 MeV.

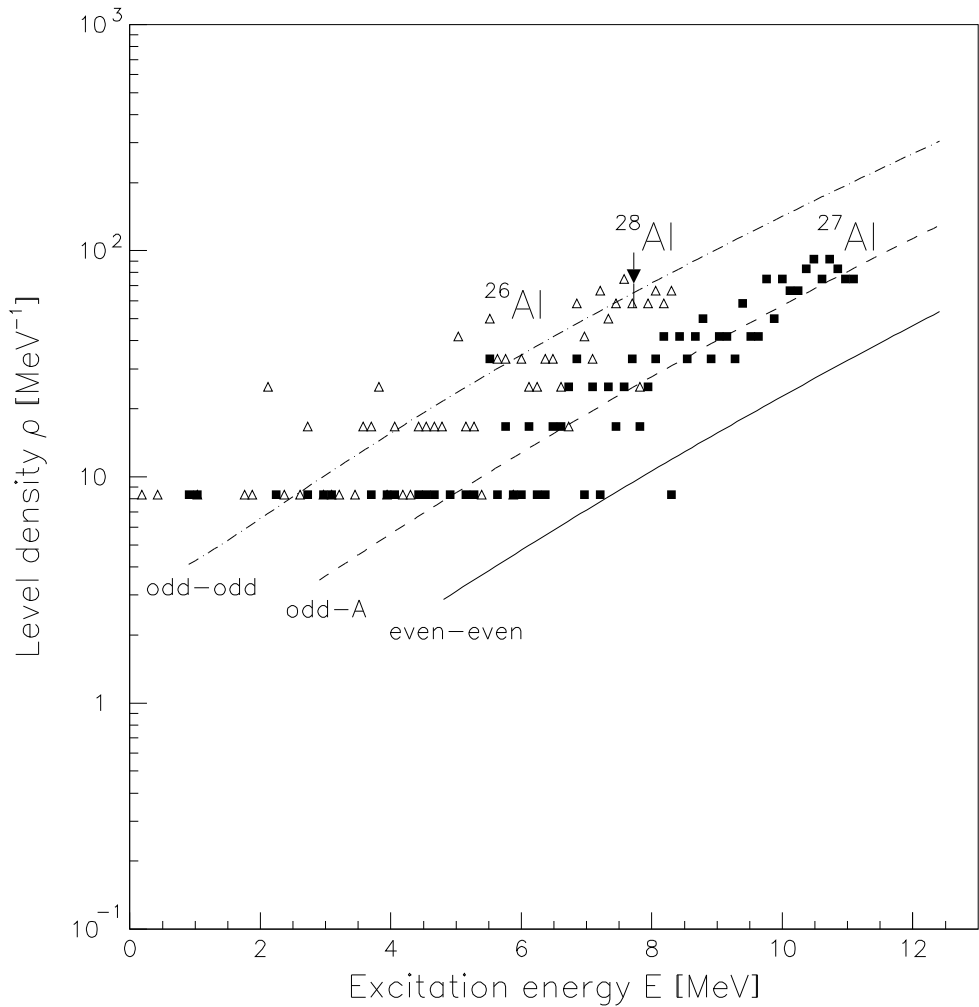


FIG. 7. Level density in ^{26}Al (open triangles) and ^{27}Al (filled squares) determined by counting the number of known levels [14] within excitation bins of 120 keV. One data point (filled triangle with error bars) is based on neutron resonance spacings in ^{28}Al [9,21]. The model calculations (curves) are performed with the same parameter set for the even-even, odd- A and odd-odd systems: $\varepsilon = 2.0$ MeV, $\Delta = 2.3$ MeV, $r = 0.56$, $A_{\text{rot}} = 0.3$ MeV, $\hbar\omega_{\text{vib}} = 5.0$ MeV and with seven proton and seven neutron pairs in the reservoir.

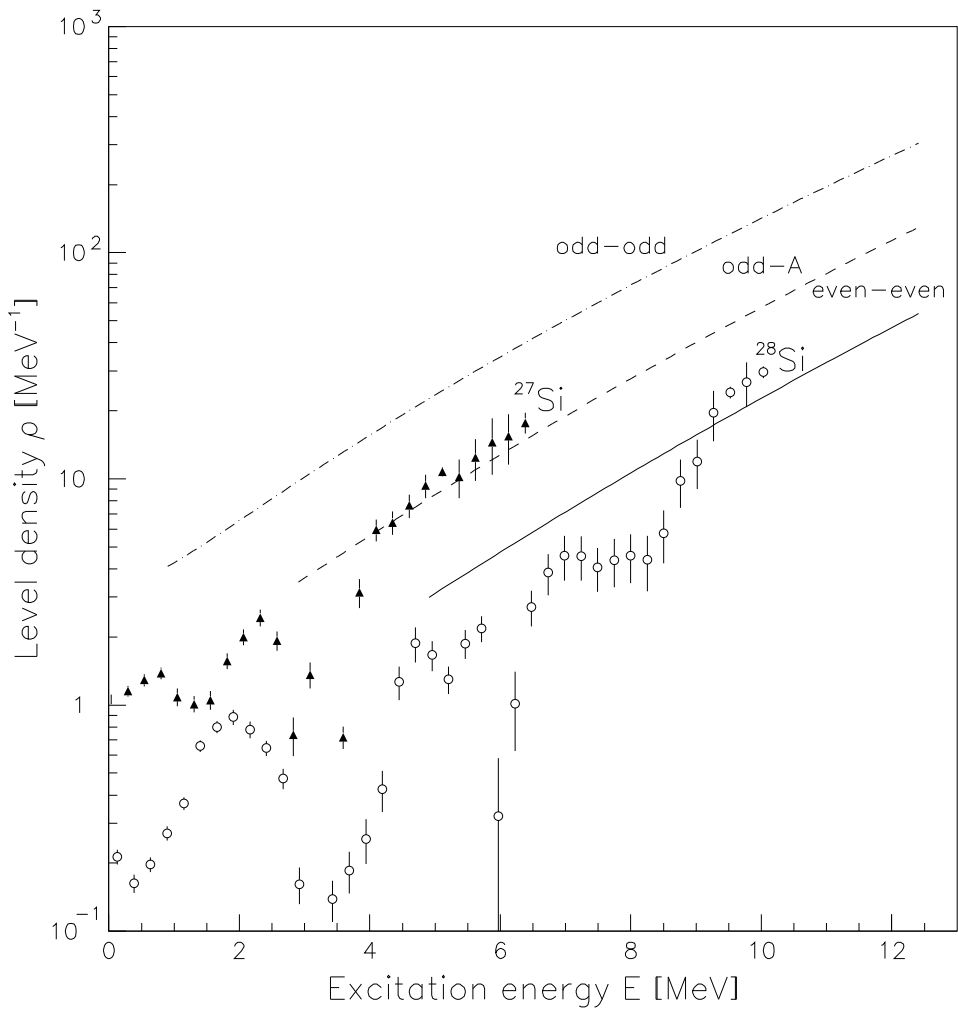


FIG. 8. Comparison between level densities extracted from primary γ -ray spectra in ^{27}Si and ^{28}Si (data points) and model predictions (curves), see text of Fig. 7.

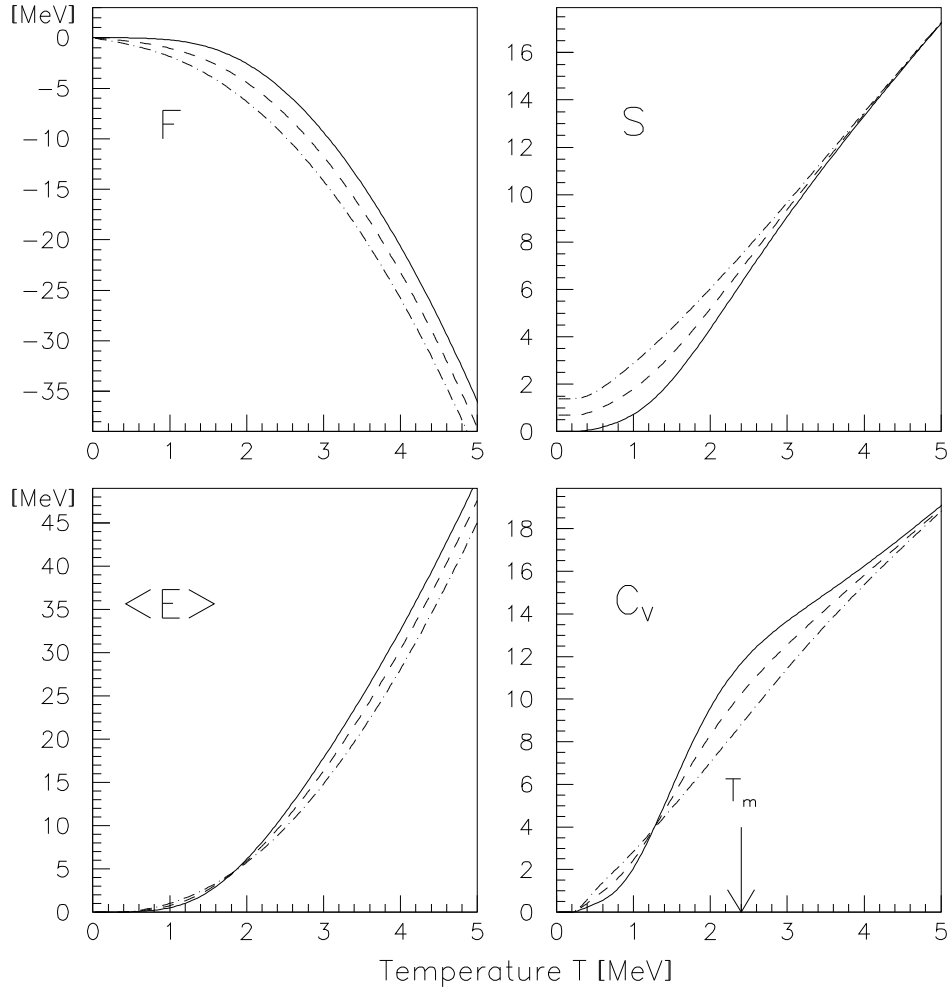


FIG. 9. Model calculations for nuclei around ^{28}Si showing even-even (solid line), odd- A (dashed line) and odd-odd (dashed-dotted line) systems. The four panels show the free energy F , the entropy S , the average excitation energy $\langle E \rangle$ and the heat capacity C_V as function of temperature T . The arrow at $T_m = 2.4$ MeV indicates the local maximum of C_V where the depairing process is strong. The parameters are given in the text of Fig. 7.

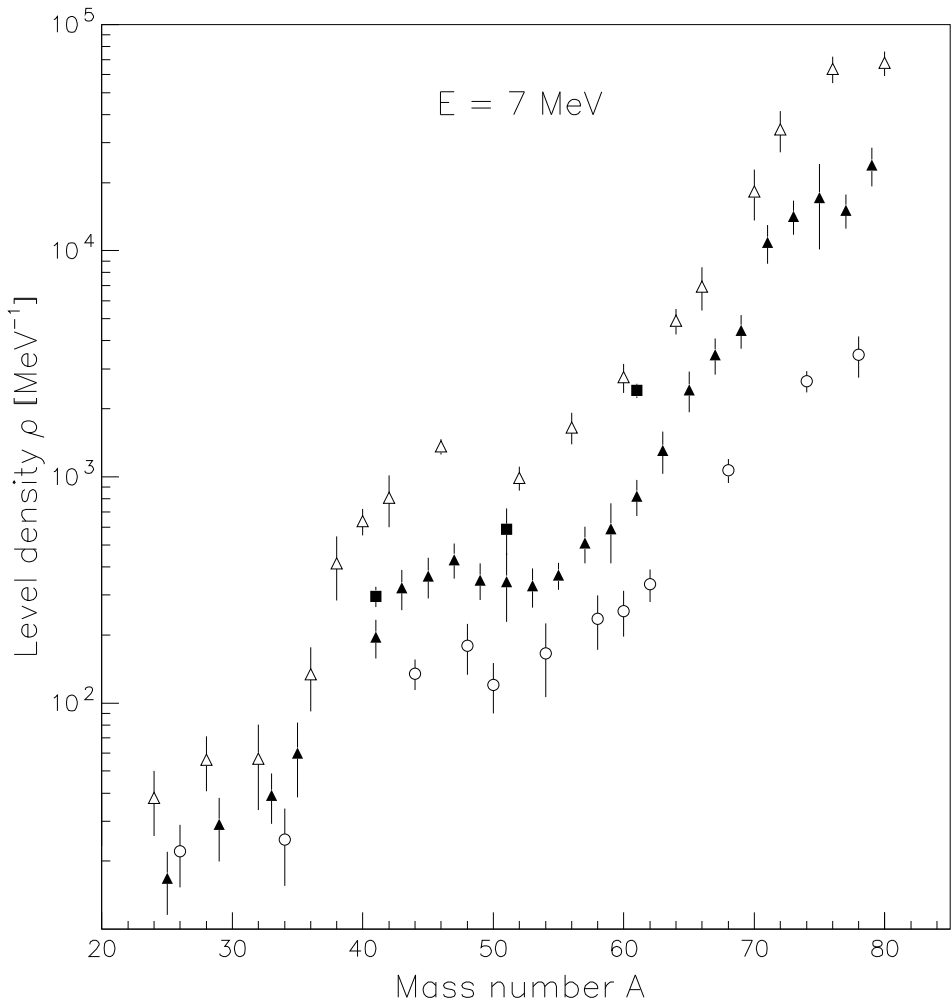


FIG. 10. Level densities as function of mass number at 7 MeV of excitation energy. The data are plotted for odd-odd (open triangles), odd-even (filled triangles), even-odd (filled squares), and even-even (open circles) nuclei. The data are extracted from experimental values, as described in Ref. [9].

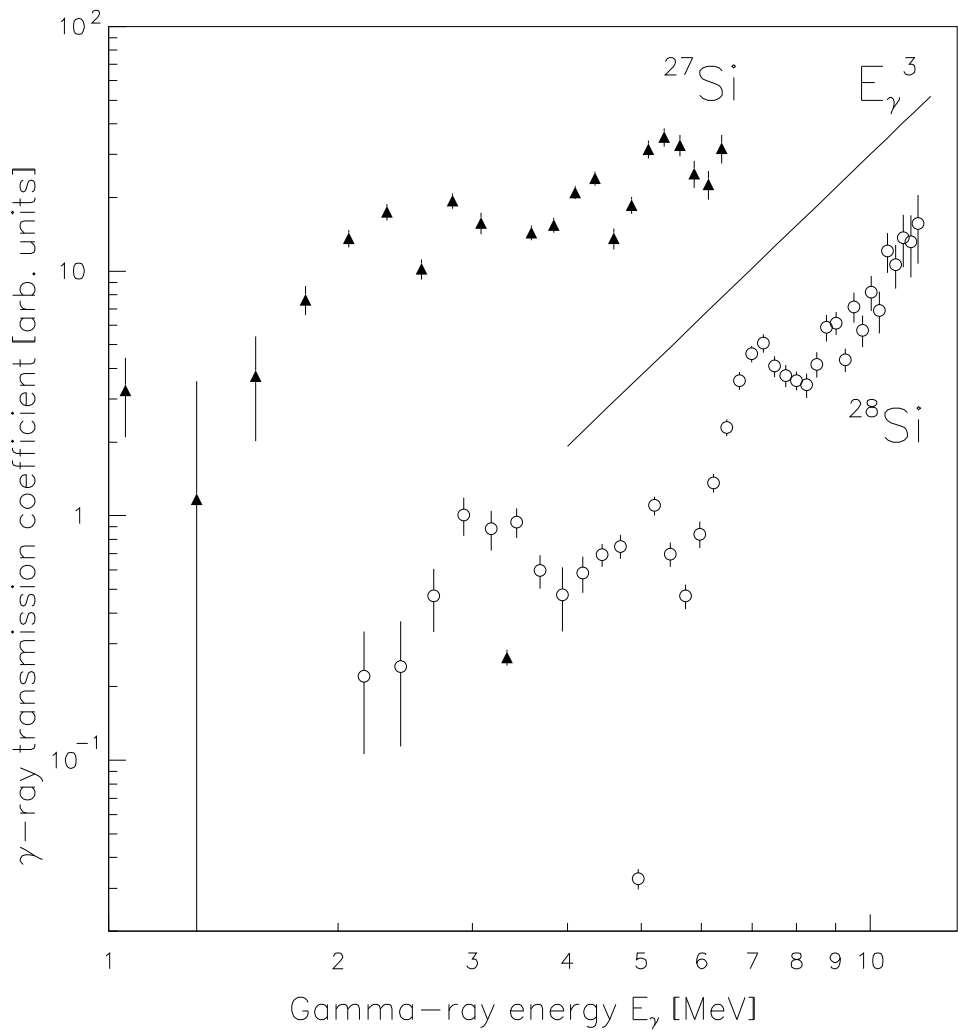


FIG. 11. Extracted γ -ray transmission coefficient $F(E_\gamma)$ in ^{27}Si and ^{28}Si . The solid E_γ^3 -line (not normalized) indicates the shape expected for single particle dipole transitions.